

Structure-related transport properties of A-site ordered perovskite $\text{Sr}_3\text{ErMn}_{4-x}\text{Ga}_x\text{O}_{10.5-d}$

W. Kobayashi[†]

Waseda Institute for Advanced Study, Waseda University, Tokyo 169-8050, Japan

T. Ishibashi

Department of Physics, Waseda University, Tokyo 169-8555, Japan

(Dated: December 5, 2018)

We report x-ray diffraction, resistivity, thermopower, and magnetization of $\text{Sr}_3\text{ErMn}_{4-x}\text{Ga}_x\text{O}_{10.5-d}$, in which A-site ordered tetragonal phase appears above $x = 1$, and reveal that the system exhibits typical properties seen in the antiferromagnetic insulator with Mn^{3+} . We succeed in preparing both A-site ordered and disordered phases for $x = 1$ in different preparation conditions, and observe a significant decrease of the resistivity in the disordered phase. We discuss possible origins of the decrease focusing on the dimensionality and the disordered effect.

I. INTRODUCTION

Perovskite oxide is denoted as ABO_3 , where A and B represent lanthanide (and/or alkaline earth elements) and transition-metal elements, respectively. B ion is surrounded by six oxygen ions, and BO_6 octahedron is formed. The octahedron mainly contributes electrical and magnetic properties of the perovskite oxide. According to the ionic radius of A ion, the bond angle $\angle B\text{-O-B}$ deviates from 180° , which causes a change of the bandwidth. In a substituted system of $R_{1-x}A_x^{2+}\text{BO}_3$, the carrier concentration is also controlled as well as the bandwidth.

The A-site ordered manganese oxide $R\text{BaMn}_2\text{O}_6$ (R : lanthanide) has attracted much attention because of significant physical phenomena such as the large magnetoresistance of 1,000 % at room temperature [2], charge and orbital orderings at high temperatures [3]. These properties attribute to A-site ordering working as "a periodic" Coulomb potential which stabilizes charge, spin, and/or orbital orderings of the electrons on B-site [4]. Owing to the randomness, A-site disordered phase of $R_{0.5}\text{Ba}_{0.5}\text{MnO}_3$ displays the spin-glass state or the itinerant ferromagnetic state instead of the charge ordered state seen in the ordered phase [3, 5].

The A-site ordered cobalt oxide $\text{Sr}_3\text{YCo}_4\text{O}_{10.5}$ also exhibits peculiar magnetic properties with a high ferromagnetic (ferrimagnetic) transition temperature of 335 K [6], which is in contrast with a spin state crossover near 100 K in LaCoO_3 [7]. In this compound, the A-site ordering stabilizes oxygen deficient ordering, which makes a volume of the CoO_6 octahedron larger than that of LaCoO_3 [8] and gives a different coordination number of Co^{3+} from LaCoO_3 . These modifications stabilize high-spin and/or intermediate-spin states of Co^{3+} even at low temperatures, which causes the peculiar magnetic properties. Hence, partial substitution for the A-site or B-site cations strongly affects the spin state leading to significant suppression of the magnetic order; Ca substitution for Sr site [9] and 6%-Mn doping in the B site [10] destroys the room-temperature ferromagnetism of $\text{Sr}_3\text{YCo}_4\text{O}_{10.5}$.

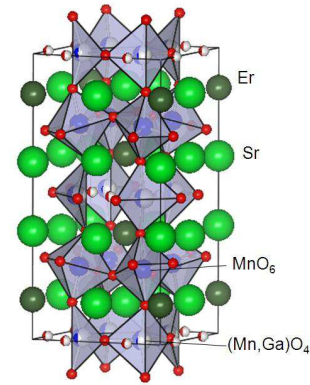


FIG. 1: (Color online) Crystal structure of $\text{Sr}_3\text{ErMn}_{4-x}\text{Ga}_x\text{O}_{10.5-d}$ ($x \geq 1$).

Recently, a new A-site ordered perovskite $\text{Y}_{0.8}\text{Sr}_{2.2}\text{Mn}_2\text{GaO}_{7.9}$ ($\text{Sr}_{2.93}\text{Y}_{1.07}\text{Mn}_{2.66}\text{Ga}_{1.34}\text{O}_{10.53}$) was reported by Gillie *et al.* [11], which is isostructural to $\text{Sr}_3\text{YCo}_4\text{O}_{10.5}$ [12, 13]. As shown in Fig. 1, this compound has an octahedral site where Mn^{3+} ions mainly occupy with about 10%-Ga ions intermixed and a tetrahedral site where both Mn^{3+} and Ga^{3+} ions occupy. They found an antiferromagnetic state below 100 K in this material showing that $\text{Y}_{0.8}\text{Sr}_{2.2}\text{Mn}_2\text{GaO}_{7.9}$ was a antiferromagnetic insulator, however, they did not report the transport properties. We have prepared polycrystalline samples of $\text{Sr}_3\text{ErMn}_{4-x}\text{Ga}_x\text{O}_{10.5-d}$ ($x = 0, 0.5, 1, 2$) where d represents oxygen deficiency and investigated the transport and magnetic properties in relation to the structure. We have succeeded in preparing both A-site ordered and disordered phases for $x = 1$ using different preparation conditions and observe a significant decrease of the resistivity in the disordered phase. We attribute this to a change of dimensionality in conduction and/or A-site disordered effect. This material can be a good playground to study order-disorder effect on the electronic states of the antiferromagnetic insulator with Mn^{3+} .

II. EXPERIMENTS

Polycrystalline samples of $\text{Sr}_3\text{ErMn}_{4-x}\text{Ga}_x\text{O}_{10.5-d}$ ($x = 0, 0.5, 1, \text{ and } 2$) were prepared by a solid state reaction. Stoichiometric amounts of SrCO_3 , Er_2O_3 , Mn_3O_4 , and Ga_2O_3 were mixed, and the mixture was sintered at 1250°C for 12 h for $x = 0$ and 0.5, 6 h for $x = 1$ and 2 in N_2 flow (100 – 200 ml/min). Then, the product was finely ground, pressed into a pellet, and sintered at 1250°C for 12 h for $x = 0$, 24 h for $x = 0.5$, and 10 h for $x = 1$ and 2 in N_2 flow (100 – 200 ml/min). The second process was repeated 2 times for $x = 0.5$, and once for $x = 1$ and 2 with intermediate grindings and pelletizings. As shown in Fig. 2(c), $x = 1$ sample exhibits A-site ordered structure. We sintered the $x = 1$ sample again using the second process, and found the sample shows a disordered structure shown in Fig. 3.

The x-ray diffraction of the sample was measured using a standard diffractometer with $\text{Cu K}\alpha$ radiation as an x-ray source in the $\theta - 2\theta$ scan mode. The structural simulations were performed using a RIETAN-2000 program [14]. The resistivity was measured by a four-probe method in a liquid He cryostat. The thermopower was measured using a steady-state technique in a liquid He cryostat with copper-constantan thermocouple to detect a small temperature gradient of about 1 K/cm. The magnetization was measured from 5 to 400 K by a commercial superconducting quantum interference device (SQUID, Quantum Design MPMS).

III. RESULTS AND DISCUSSION

Figure 2 shows the x-ray diffraction patterns of $\text{Sr}_3\text{ErMn}_{4-x}\text{Ga}_x\text{O}_{10.5-d}$ ($x = 0, 0.5, 1, \text{ and } 2$). All the peaks are indexed as a cubic cell of the space group $Pm\bar{3}m$ with the lattice parameter of $a \sim 3.8$ and 3.85 \AA for $x = 0$ and 0.5, respectively. This cubic cell is also seen in $\text{Sr}_{1-x}\text{Y}_x\text{CoO}_{3-\delta}$ with small x [6]. With increasing Ga content x , crystal structure changes from the cubic perovskite to a tetragonal A-site ordered perovskite (space group: $I4/mmm$, Fig. 1) with the lattice parameter of $a \sim 7.63$ and 7.65 \AA , and $c \sim 15.58$ and 15.56 \AA for $x = 1$ and 2, respectively. This result is consistent with the structural analysis by Gillie *et al.* [11]. As shown in the inset of Fig. 2(d), superstructure peaks corresponding to the A-site ordering are observed, while they do not appear for $x = 0$ and 0.5 samples. Ga ions selectively occupy the tetrahedral site to stabilize the A-site ordered structure as shown in Fig. 1 [11]. Thus, $x = 1$ is a minimal amount to stabilize the structure. Gillie *et al.* reported that the oxygen content of $\text{Sr}_2\text{YMn}_2\text{GaO}_{7.9}$ is 7.9 showing formal valence of Mn ion is almost $3+$. Thus, it is assumed that the formal valence of Mn ion is also $3+$ in the ordered compounds presented here.

Figure 3 shows the x-ray diffraction patterns of $\text{Sr}_3\text{ErMn}_3\text{GaO}_{10.5-d}$ with different preparation conditions. Obviously, two patterns are different; one sam-

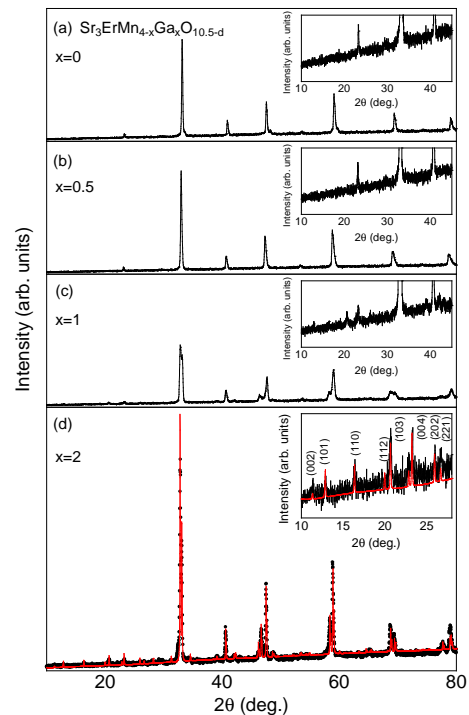


FIG. 2: (Color online) (a)-(d) X-ray diffraction patterns of $\text{Sr}_3\text{ErMn}_{4-x}\text{Ga}_x\text{O}_{10.5-d}$ ($x = 0, 0.5, 1, \text{ and } 2$). The insets represent the magnified x-ray patterns at low angles. The red line of the inset of Fig. 2(d) represents a simulated pattern.

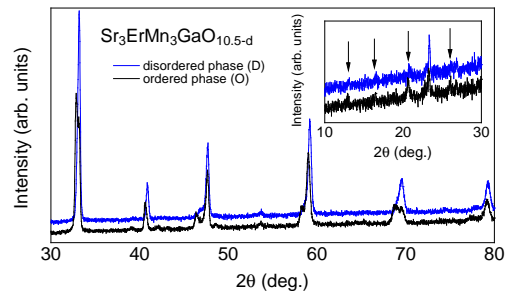


FIG. 3: (Color online) X-ray diffraction patterns of ordered and disordered $\text{Sr}_3\text{ErMn}_3\text{GaO}_{10.5-d}$. The inset represents the magnified x-ray pattern at low angles.

ple was identified to the tetragonal ordered phase (hereafter this is denoted by O sample), and the other was identified to the disordered-cubic perovskite phase (D sample). Similar structures are originally found in $\text{RBaMn}_2\text{O}_6/\text{R}_{0.5}\text{Ba}_{0.5}\text{MnO}_3$ systems [3]. We would like to say that the O sample is metastable so that the longer sintering stabilizes the disordered phase. Thus, this composition is just on the verge of order and disorder. As shown in the inset of Fig. 3, the superstructure peaks of D sample are hardly visible.

Figure 4 (a) shows the thermopower of $\text{Sr}_3\text{ErMn}_{4-x}\text{Ga}_x\text{O}_{10.5-d}$ ($x = 0, 0.5, 1, \text{ and } 2$). The magnitude of the thermopower is between 60 and 110

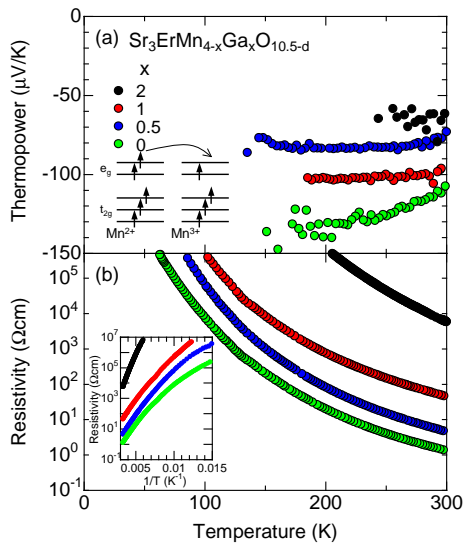


FIG. 4: (Color online) (a) Thermopower and (b) resistivity of $\text{Sr}_3\text{ErMn}_{4-x}\text{Ga}_x\text{O}_{10.5-d}$ ($x=0, 0.5, 1$, and 2).

$\mu\text{V/K}$, and the sign is negative showing that the carriers are electrons. Assuming that the formal Mn valence is $3+$, we expect that a tiny amount of electrons on Mn^{2+} moves in the background of Mn^{3+} as shown in the inset of Fig. 4(a). Using an extended Heikes formula [15], the valence of Mn ion was evaluated to be $2.71+$ at 300 K corresponding to $d = 0.43$ for $x = 1$ sample with spin degeneracy term of $g_{\text{Mn}^{2+}} = 6$ and $g_{\text{Mn}^{3+}} = 5$.

Figure 4 (b) shows the resistivity of $\text{Sr}_3\text{ErMn}_{4-x}\text{Ga}_x\text{O}_{10.5-d}$ ($x = 0, 0.5, 1$, and 2). Semiconducting temperature dependence is observed for all the samples. With x , the magnitude of the resistivity decreases mainly due to decrease of scattering centers of the Ga ions. As seen in the inset of Fig. 4(b), the temperature dependence is described by an activation-type conduction $\rho = \rho_0 \exp(\frac{E_g}{k_B T})$ where E_g represents activation energy above 200 K . The activation energy E_g was evaluated to be $0.133, 0.146, 0.149$, and 0.246 eV for $x=0, 0.5, 1$, and 2 , respectively.

Figure 5(a) shows the magnetization of $\text{Sr}_3\text{ErMn}_{4-x}\text{Ga}_x\text{O}_{10.5-d}$ ($x = 0, 0.5, 1$, and 2). As shown in Figs. 5(b) and (c), the data was fitted by the Curie-Weiss law described by $\chi = \frac{C}{T - \theta_W} + \chi_0$, where C , θ_W , and χ_0 represent Curie constant, Weiss temperature and temperature independent term of the magnetic susceptibility, respectively. C was evaluated to be $0.023, 0.019, 0.026$, and $0.018\text{ emu/K}\cdot\text{g}$ for $x = 0, 0.5, 1$, and 2 , corresponding to $12.34, 11.14, 13.17$, and $11.07\text{ } \mu_B/\text{f.u.}$, respectively. These values are roughly explained by coexistence of $9.6\text{ } \mu_B$ of Er^{3+} with $g = \frac{6}{5}$ and $J = \frac{15}{2}$ and $3.87\text{ } \mu_B$ and $4.90\text{ } \mu_B$ in the high-spin states of Mn^{4+} and Mn^{3+} . χ_0 was evaluated to be $1.39 \times 10^{-5}, 1.57 \times 10^{-5}, 0$, and 0 emu/g for $x = 0, 0.5, 1$, and 2 samples, respectively. Since $x = 0$ and 0.5 samples show relatively good electric conductance compared with those

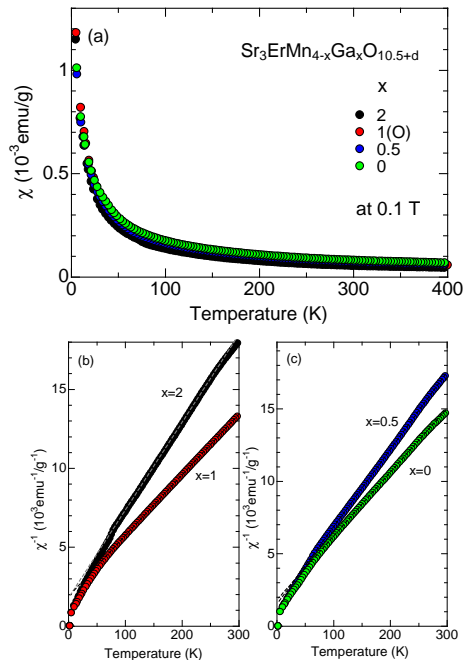


FIG. 5: (Color online) Magnetic susceptibility of $\text{Sr}_3\text{ErMn}_{4-x}\text{Ga}_x\text{O}_{10.5-d}$ ($x = 0, 0.5, 1$, and 2). The inset shows inverse susceptibility.

of $x = 1$ and 2 samples, this contribution may come from conducting electrons. All the samples exhibit negative θ_W ($-45, -29, -52$, and -30 K for $x = 0, 0.5, 1$, and 2 , respectively) implying antiferromagnetic interaction in this system. At around 60 K , the slope of χ^{-1} changes showing an existence of magnetic anomaly for all the samples. Since the antiferromagnetism was observed in $\text{Sr}_2\text{YMn}_2\text{GaO}_8-d$ below 100 K [11], the anomaly at around 60 K in $\text{Sr}_3\text{ErMn}_{4-x}\text{Ga}_x\text{O}_{10.5-d}$ can be also related to antiferromagnetic order of Mn^{3+} .

Lastly, we will discuss a difference of the transport and magnetic properties between the ordered (O sample) and disordered samples (D sample). Figure 6 (a) shows the temperature dependences of the resistivity of the O and D samples. The magnitude of the resistivity of the D sample is one order of magnitude smaller than that of the O sample, while the thermopower and magnetization of the D sample quite resemble those of the O sample as seen in Fig. 6(b). This strongly contrasts with the difference between the ferromagnetic-metal state of the disordered $R_{0.5}\text{Ba}_{0.5}\text{MnO}_3$ and charge-ordered insulating state of the ordered $R\text{BaMn}_2\text{O}_6$ [3]. This variety of the properties comes from $\text{Mn}^{3.5+}$ with the charge degree of freedom, while $\text{Sr}_3\text{ErMn}_{4-x}\text{Ga}_x\text{O}_{10.5-d}$ has Mn^{3+} without the charge degree of freedom causing the small difference between the properties.

The difference of the resistivity shown in Fig. 6(a) is explained by several possible origins as follows: (1) a decrease of the carrier concentration, (2) an increase of the scattering time, (3) a change of dimensionality in con-

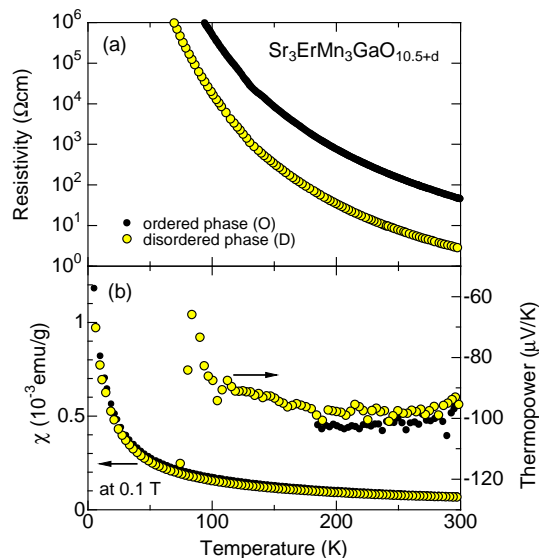


FIG. 6: (Color online) (a) Resistivity and (b) thermopower and magnetization of the ordered and disordered phases.

duction and (4) a change of electronic structure induced by the disordering of A site. As seen in Fig. 6(b), two samples exhibit almost the same magnitude of the thermopower of $-100 \mu\text{V}/\text{K}$. Since thermopower is a function of carrier concentration, the result shows that carrier concentration does not differ so much in the two samples. In addition, since the content x of Ga ions which can be scattering centers is 1 in both samples, a possibility of (2) can be also denied. As stated in the introduction, Ga ion selectively occupies tetrahedral sites in the O phase, while Ga and Mn ions randomly occupies in the D phase. Thus, a dimensionality in conduction can change from 2D in the O sample to 3D in the D sample, which can be a possible origin of the decrease of the resistivity. Another possi-

bility is a change of electronic structure induced by the disordering of A site. A-site disordering generally induces a random potential in a perovskite oxide, which may affect the electronic structure of the material. Indeed, it is theoretically found that the introduced random potential in the Hubbard Hamiltonian causes an antiferromagnetic metallic phase instead of the antiferromagnetic insulating state [16]. Although the origin of the difference of the resistivity is not clear at present, this system can be a good playground for investigating A-site disorder effect on antiferromagnetic insulator with Mn^{3+} .

IV. SUMMARY

In summary, we have measured x-ray diffraction, resistivity, thermopower, and magnetization of $\text{Sr}_3\text{ErMn}_{4-x}\text{Ga}_x\text{O}_{10.5-d}$ system, in which A-site ordered tetragonal phase appears above $x = 1$, and observed large negative thermopower, semiconducting conduction, and magnetic susceptibility with a kink at 60 K implying antiferromagnetism. We succeed to prepare both A-site ordered and disordered phases for $x = 1$ sample and observe a significant decrease of the resistivity in the disordered phase. We attribute this to a change of dimensionality in conduction and/or a change of electronic structure induced by the disordering of A sites.

V. ACKNOWLEDGEMENTS

We acknowledge I. Terasaki for fruitful discussion. This study was supported by the program entitled "Promotion of Environmental Improvement for Independence of Young Researchers" under the Special Coordination Funds for Promoting Science and Technology provided by MEXT, Japan.

[[†]] email address: kobayashi-wataru@suou.waseda.jp

- [2] T. Nakajima and Y. Ueda, *J. Appl. Phys.* **98** (2005) 46108.
 [3] T. Nakajima, H. Kageyama, H. Yoshizawa and Y. Ueda, *J. Phys. Soc. Jpn.* **71** (2002) 2843.
 [4] Y. Motome, N. Furukawa, and N. Nagaosa, *Phys. Rev. Lett.* **91** (2003) 167204.
 [5] D. Akaoshi, M. Uchida, Y. Tomioka, T. Arima, Y. Matsui, and Y. Tokura, *Phys. Rev. Lett.* **90** (2003) 177203.
 [6] W. Kobayashi, S. Ishiwata, I. Terasaki, M. Takano, I. Grigoraviciute, H. Yamauchi, and M. Karppinen, *Phys. Rev. B* **72** (2005) 104408.
 [7] K. Asai, O. Yokokura, N. Nishimori, H. Chou, J. M. Tranquada, G. Shirane, S. Higuchi, Y. Okajima, and K. Kohn, *J. Phys. Soc. Jpn* **50** (1994) 3025.
 [8] S. Ishiwata, W. Kobayashi, I. Terasaki, K. Kato, and M. Takata, *Phys. Rev. B* **75** (2007) 220406.
 [9] S. Yoshida, W. Kobayashi, T. Nakano, I. Terasaki, K.

- Matsubayashi, Y. Uwatoko, I. Grigoraviciute, M. Karppinen, and H. Yamauchi, (submitted).
 [10] W. Kobayashi, S. Yoshida, and I. Terasaki, *Prog. Solid State Chem.* **35** (2007) 355.
 [11] L. J. Gillie, H. M. Palmer, A. J. Wright, J. Hadermann, G. Van Tendeloo, and C. Greaves, *J. Phys. Chem. Solids* **65** (2004) 87.
 [12] S. Ya. Istomin, J. Grins, G. Svensson, O. A. Drozhzhin, V. L. Kozhevnikov, E. V. Antipov, and J. P. Attfield, *Chem. Mater.* **15** (2003) 4012
 [13] R. L. Withers, M. James, and D. J. Goosens, *J. Solid State. Chem.* **174** (2003) 198.
 [14] F. Izumi and T. Ikeda, *Mater. Sci. Forum* **198** (2000) 321.
 [15] W. Koshibae, K. Tsutsui, and S. Maekawa, *Phys. Rev. B* **62** (2000) 6869.
 [16] H. Shinaoka, and M. Imada, *Phys. Rev. Lett.* **102** (2009) 016404.